ELSEVIER

Journal of Power Sources 65 (1997) 81–85

JOURNAL OF POWER SOURCES

13

Electrochemical performance of gelled zinc alloy powders in alkaline solutions

Jean-Yves Huot *, Emmanuelle Boubour

Noranda Advanced Materials, c/o Noranda Technology Centre, 240 Hymus Blvd, Pointe-Claire, Que., H9R 1G5, Canada

Received 4 November 1996; accepted 27 November 1996

Abstract

The electrochemical performance of gelled zinc powders was investigated at various discharge rates and temperatures. Pure zinc powder does not perform well, and fast passivation is clearly evident at 100 mA g^{-1}. Material utilization of zinc powder was found to increase with the addition of lead, bismuth, calcium and aluminum to pure zinc powder. The addition of indium only affected electrical performance at extremely high rates. The presence of fine zinc particles had a marginal effect on the material utilization of zinc alloys. The effects of high temperature storage and low temperature anodic discharge were also investigated.

Keywords: Zinc electrodes/gelled; Electrolytes/aqueous

1. Introduction

Mercury-free alkaline Zn–MnO_2 batteries were first marketed in the early 1990s. The reduction and the ultimate elimination of mercury in zinc anodes first impacted on cell performance, such as shock and vibration sensitivity, zinc gassing and the corresponding risk of cell leakage, and lower capacity or service at room and low temperatures [1]. The latest mercury-free technologies were however strongly improved by new zinc alloys and new zinc anode formulations [2].

The performance of the zinc electrodes can also be assessed by out-of-cell testing, such as gassing [3,4], resistivity [3] and service [3,5] tests. For instance, these methods clearly revealed the effect of iron on after-discharge gassing, shock sensitivity of mercury-free gelled anodes, as well as alloying effects on anode gassing, which were also detected in mercury-free alkaline cells.

This study is entirely devoted to the effects of physico-chemical properties of alloys, as well as storage conditions of gelled anodes, on out-of-cell capacity of zinc as measured by anodic discharge at room temperature. The physico-chemical properties of interest were the chemical composition and particle size distribution of zinc powder. The ultimate goal was to estimate the specific contribution of zinc powder to cell performance in the absence of any additives in the gelled anode.

2. Experimental

Battery grade zinc powders were made by proprietary gas atomization of 99.997% molten zinc. Alloying elements (99.99%) were added to the molten zinc. These powders were classified and characterized by the usual techniques, namely sieve analysis, chemical analysis (flame-AA), gassing tests, density measurements, and scanning electron microscopy (SEM, Weiss apparatus). The typical sieve analysis was as follows:

+30 mesh	−30, +60	−60, +100	−100, +140	−140, +200	−200 mesh
0	22%	30%	20%	20%	8%

Galvanostatic discharge tests at 100, 250, 500 and 1500 mA g^{-1} (zinc) were performed in a three-electrode Plexiglass electrochemical cell at room temperature with a Solartron 1286 potentiostat. The zinc anode, weighing about 1.6 g, in contact with a brass collector, was surrounded by a 100 mesh Nylon separator. The anodic size roughly corresponds to 'AAA' (LR03) size. The counter-electrode was made from nickel, and the reference electrode was Hg/HgO/37 wt.% KOH–3 wt.% ZnO. Unless otherwise mentioned, zinc paste contained 65 wt.% zinc powder, 34.5 wt.% KOH solution and 0.5 wt.% Carbopol 940. The alkaline solution used was 37 wt.% KOH containing 3 wt.% ZnO, and the electrode potential was given with respect to Hg/HgO. The depth of discharge (DOD) is expressed as a percentage of the theoretical zinc anode capacity, i.e. 820 mAh g^{-1}. Here, Pb–Zn

* Corresponding author.

PII S0378-7753(96)02613-4

refers to Pb(500 ppm)–Zn, 6%Hg–Pb–Zn refers to amalgamated Pb–Zn, ABI refers to Al–Bi–In, BIC refers to Bi–In–Ca, and AB refers to Al–Bi alloys.

3. Results

3.1. Continuous discharge of zinc anode

An anodic discharge test of porous zinc electrodes was performed in both the electrochemical cell and a C-size cell. A commercial C-size cell was opened, its zinc anode was removed and a new one was fitted. The collector was reinstalled without sealing the cell. Fig. 1 shows that the material utilization is lower, but voltage is higher, in a C-size cell as compared to an AAA-size electrochemical cell. The initial E–mAh g^{-1} curve in a C-size cell does not show any E–$t^{0.5}$ effect associated with some mass transfer within the anode itself [4]. This E–$t^{0.5}$ effect only occurred in electrochemical cells [4,6]. The linear discharge curve of zinc in a C-size cell might be ascribed to a gradual increase in ohmic drop, as this slope is equivalent to that of the final part of the discharge curve (in the electrochemical cell) that was assigned to an ohmic contribution [6].

The relative performance of various zinc alloys in rebuilt C-size cells and in the AAA-size electrochemical cell at 100 mA g^{-1} displayed almost the same trends, with higher capacity for Pb–Zn and Bi–Zn alloys (Table 1). The much lower mass utilization in a C-size cell was not expected when compared to the AAA-size cell [7]. In the absence of any fundamental advantage in using the real alkaline cell, the performance assessment was only done in the AAA-size electrochemical cell.

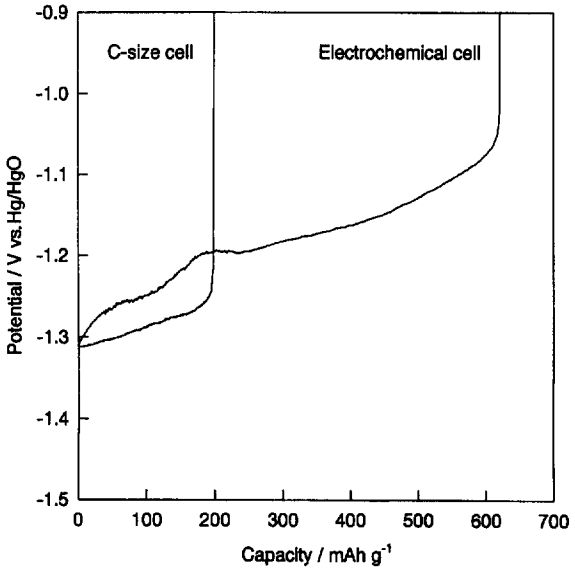

Fig. 1. Discharge curve of Pb–Zn at 100 mA g^{-1} in rebuilt C-size and an electrochemical cell at room temperature.

Table 1
Relative performance of various zinc alloys down to −1.1 V (vs. Hg/HgO) in rebuilt C-size cells and in AAA-size electrochemical cell at 100 mA g^{-1}

Zinc alloy	Rebuilt C-size cell	Electrochemical cell
Pure zinc	100% (140 mAh g^{-1})	100% (416 mAh g^{-1})
In(500)–Zn	107%	84%
Pb(500)–Zn	143%	122%
Bi(125)–Zn	114%	153%

3.2. Continuous discharge at 100 mA g^{-1}

3.2.1. Effect of chemical composition

Anodic discharge of single, binary and ternary zinc alloys was performed at 100 mA^{-1}. Table 2 shows that that pure zinc did not perform well, while the addition of one alloying element improved performance in increasing order In < Pb < Bi.

Chemical effects were also observed on the amperage of D-size cells, where lead and indium strongly improved performance, while an excess of bismuth reduced amperage [8]. This was explained by lead's and indium's ability to improve particle to particle contact.

The effect of alloying elements was still evident in binary alloys, while more complex effects appeared to occur in ternary alloys (Table 2). There was some evidence that aluminum also increased zinc utilization in continuous discharge. Those relative effects on performance are quite different from the inhibiting action of those elements [9]. The effect of the Bi:Al ratio (AB zinc alloys) and the Al:Bi:In ratio (ABI zinc alloys) on electrical performance was also investigated (Table 3).

Again, bismuth was found to improve performance in continuous discharge of AB and ABI alloys, without inducing any dips on the discharge curve. The effect of aluminum is small and it is not consistent. Typical discharge curves of ABI and AB zinc anodes are displayed in Fig. 2.

Table 2
Anodic discharge performance of zinc alloys in an AAA-size electrochemical cell at the end point voltage of −1.1 V (vs. Hg/HgO), initial slope (E–$t^{0.5}$), plateau slope, and dips

Powder	Service (mA g^{-1})	Slope (V mAh^{-1} g×10^4)	E–$t^{0.5}$	Dips (mV)
Pure zinc				
Zn	297	2.8	1.4	no
Single				
In(500)	336	3.4	1.4	no
Pb(500)	508	2.9	1.3	22
Bi(500)	554	1.6	2.2	no
Binary				
Pb(500)In(500)	448	2.3	1.7	30
Bi(250)In(250)	347	5.3	1.9	no
Bi(250)Al(100)	530	1.6	2.3	no
Ternary				
Al(100)Bi(400)In(250)	499	2.4	1.8	no
Bi(500)In(500)Pb(500)	459	3.0	2.4	17
Bi(250)In(250)Ca(150)	416	0.7	n.a.	no

Table 3
Anodic discharge performance of AB and ABI zinc alloys in an AAA-size electrochemical cell at the end point voltage of −1.1 V (vs. Hg/HgO), initial slope (E–$t^{0.5}$), plateau slope, and dips

Powder	Service (mAh g^{-1})	Slope (V mAh^{-1} g × 10^4)	E–$t^{0.5}$	Dips (mV)
AB alloy				
Bi(100)Al(100)	548	1.6	1.6	no
Bi(250)Al(100)	530	1.6	2.3	no
Bi(500)Al(100)	601	1.7	1.6	no
Bi(250)Al(300)	533	2.1	2.2	no
ABI alloy				
Al(20)Bi(250)In(250)	347	5.3	1.9	no
Al(40)Bi(400)In(250)	565	1.5	n.a.	20
Al(100)Bi(400)In(250)	499	2.4	1.8	no
Al(120)Bi(450)In(250)	542	1.3	2.7	no

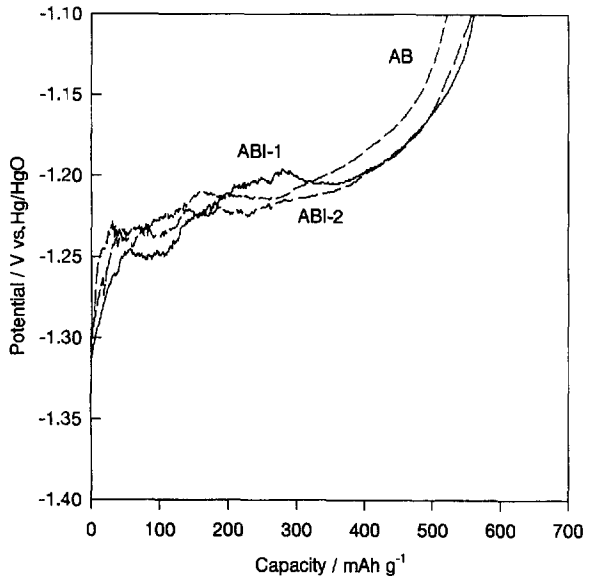

Fig. 2. Typical discharge curves of Bi(250)Al(300) or AB, Al(40)Bi(400)In(250) or ABI-1, and Al(120)Bi(450)In(250) or ABI-2 zinc anodes at 100 mA g^{-1}.

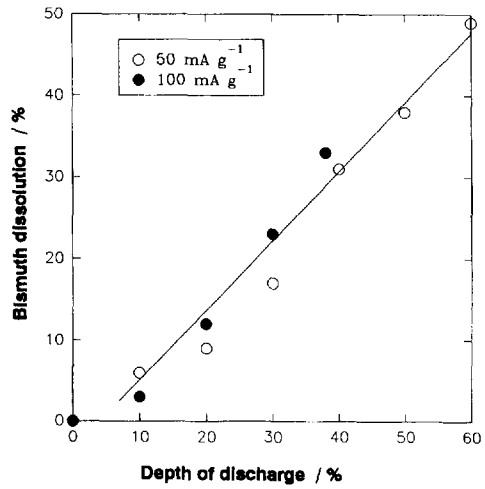

Fig. 3. Bismuth dissolution occurring at different depths of anodic discharge of ABI zinc anode. Only one linear curve was fitted at 50 and 100 mA g^{-1}.

The effect of Bi is likely due to its impact on the plateau slope (Table 1), as the plateau potential is not affected by zinc alloying. One possible mechanism might be the effect of dissolved bismuth or solid bismuth oxide on anode conductivity. As mentioned in the previous section, the linear part of the discharge curve (plateau slope) was ascribed to an ohmic contribution associated with the accumulation of zinc hydroxide–oxide within the anode pores [6,10]. Anodic dissolution of the Bi–Zn anode did result in significant Bi dissolution at 50 and 100 mA g^{-1} (Fig. 3), but Bi species were not detected in the surrounding free KOH. This is likely due to the very low solubility of bismuth salts in neutral and alkaline solutions. In other words, bismuth oxide would be mixed with the zinc hydroxide–oxide and would increase its electronic conductivity. It was previously noted that trivalent atoms, similar in size to that of zinc, increase conductivity up to 1% of the zinc oxide [11]. Such an increase in electronic conductivity should increase local material utilization by keeping more zinc particles connected to the overall electronic network.

Other possible mechanisms would be:

(i) a preferential interaction between traces of bismuth species and carboxylic groups of Carbopol 940;

(ii) the adsorption of Carbopol 940 on Bi-rich zinc surfaces;

(iii) the effect of bismuth oxide on zinc oxide film porosity and ultimate zinc passivation.

3.2.2. *Effect of particle size distribution (PSD)*

The classification of zinc powder allows us to produce various final particle size distributions from a given crude particle size distribution. Here, two types of clipping were performed with three zinc alloys, in order to get 1% and 8% less than 200 mesh. Table 4 shows that a higher –200 mesh content did not improve material utilization of zinc anodes. This is also confirmed by the In(500)–Zn material utilization of 41% when the –200 mesh fraction reached 19%.

3.2.3. *Effect of discharge and storage temperatures*

Storage at high temperatures decreases the zinc anode capacity [2,7]. After 8 days at 71°C (8 HT), service was found to drop by 10–15% in all the samples (Table 5). This agrees with the capacity retention curve of a typical alkaline cell [7]. However, zinc gassing accounts for less than 1% of the zinc loss. This means that the drop in service was not

Table 4
Effect of fines on material utilization of zinc anodes containing various zinc alloys. Fines are expressed as −200 mesh

	−200 mesh fraction	
	1%	8%
Pure Zn	52%	38%
In(500)–Zn	45%	41%
Pb(500)–Zn	64%	62%

Table 5
Room temperature (RT) service (mAh g^{-1}) after days at high temperature (HT) storage and low temperature service of fresh zinc anodes. The corresponding plateau slope is also given

Powder	Service (mAh g^{-1}, % fresh RT)			Slope (mAh g^{-1}–V × 10^4)		
	Fresh	After 8 HT	Fresh 0°C	Fresh	After 8 HT	Fresh 0°C
6% Hg–Pb–Zn	579	500, 86%	259, 45%	2.0	2.0	6.0
Pb–Zn	569	492, 86%	162, 28%	2.9	6.0	34
ABI	541	488, 90%	137, 25%	1.3	2.6	22

ABI = Al(120)Bi(450)In(250).

Table 6
High-rate discharge of various zinc anodes containing 63 wt.% zinc alloys

Powder	Rate (mA g^{-1})	Service (mAh g^{-1})	Dips (mV)	Powder	Rate (mA g^{-1})	Service (mAh g^{-1})	Dips (mV)
Pb–Zn	100	415	35	AB	100	483	no
	250	50	0–60		250	202	25
	500	13	no		500	25	no
ABI	100	410	0–30	BIC	100	416	no
	250	236	0–40		250	252	no
	500	11	no		500	13	no

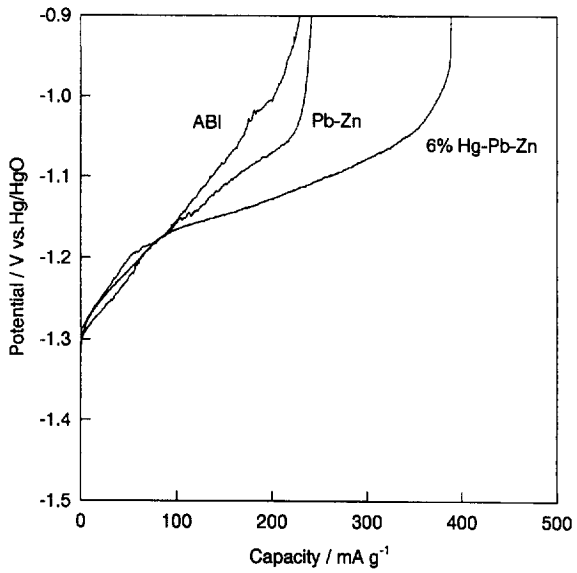

Fig. 4. Discharge curves of 6% Hg–Pb–Zn, Pb–Zn and ABI zinc anodes at 0°C. Here ABI refers to Al(120)Bi(450)In(250).

caused by zinc loss. It was more likely associated with gel degradation due to chemical reactions and water loss. The common performance drop of 6% Hg–Pb–Zn and Pb–Zn anodes is also strong evidence that zinc gassing plays a minor role, as zinc gassing is increased by a factor of ten when going from amalgamated to mercury-free zinc anodes.

The low temperature performance (fresh 0°C in Table 5) was markedly better with the amalgamated zinc anode (Fig. 4). This is likely due to the improved electronic conductivity caused by mercury interparticle bridges and patches [12]. That made the electronic network of the porous electrode more resistant to zinc oxide precipitation in pores and interparticle spaces, as mercury could not be dissolved at the zinc anode potential.

3.3. Continuous discharge at high rates

An improved high-rate performance of AA-size cells has been advertised by several battery companies in the past two years. High-rate discharge refers to rates above 200 mA g^{-1}. The high-rate performance at 250 mA g^{-1} was very poor with Pb–Zn, while it was slightly higher with BIC powder (Table 6).

The material utilization under very high-rate anodic discharge at 500 mA g^{-1} was very low because the common end point voltage of −1.1 V did not take into account the larger ohmic drop. Hence, the cut-off was located near the initial part of the discharge curve.

The extremely high-rate anodic discharge of pure zinc at 1.5 A g^{-1} showed a linear decrease in voltage that was faster for the lower fines content (Fig. 5). This performance under such extreme conditions was not improved by alloying with Pb and In. This linear behavior suggests some fast passivation and ohmic contribution due to local zincate supersaturation around zinc particles.

3.4. Intermittent discharge

Partial anodic discharge, up to 50% of the measured total capacity under continuous discharge at 100 mA g^{-1}, followed by a 20 h rest, and further anodic discharge to −0.8 V displayed higher performance when compared to the continuous discharge (Table 7). On the other hand, the replacement of mercury and lead by Al, Bi and In did not affect

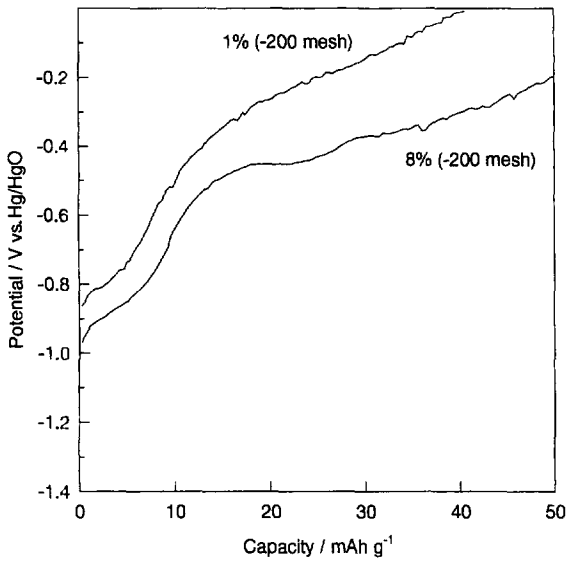

Fig. 5. Discharge curves of pure zinc powders at 1.5 A g^{-1} at room temperature.

Table 7
Intermittent and continuous discharge of amalgamated and lead-free zinc alloys at 100 mA g^{-1}

Powder	Service (mAh g^{-1})	
	Continuous	Intermittent
6% Hg–Pb–Zn	579	693
Al(120)Bi(450)In(250)	541	645
Al(50)Bi(450)In(200)	437	515

either the intermittent or the continuous discharge characteristics, while the chemical composition of ABI powder did.

4. Conclusions

The electrochemical performance of gelled zinc powder was investigated at various discharge rates and temperatures. Pure zinc powder does not perform well, and fast passivation is clearly evident at 100 mA g^{-1}. The material utilization of zinc powder was found to increase with the addition of lead, bismuth, calcium and aluminum to pure zinc powder. The effect of bismuth was associated with the dissolution–precipitation of bismuth oxide and its effect on zinc oxide–hydroxide conductivity accumulated in anode pores. The addition of indium did not impact on electrical performance at any rates. The presence of fine zinc particles had a marginal effect on the material utilization of zinc alloys. Storage at high temperatures decreased material utilization of amalgamated, lead–zinc and lead-free alloys by the same extent. This was attributed to a gel deterioration, rather than a zinc loss due to excessive zinc gassing. Low temperature anodic performance strongly depends on the presence of mercury, while the difference in the performance of mercury-free alloys is negligible.

Acknowledgements

The authors thank Daniel Marcotte for performing the anodic discharge tests of Table 6.

References

[1] D. von Borstel and D.H. Spahrbier, *Prog. Batteries Battery Mater., 10* (1991) 38.
[2] T. Messing, *IECEC Conf., 1* (1993) 1079.
[3] J.Y. Huot, in A. Attewell and T. Keily (eds.), *Power Sources 14*, International Power Sources Symposium, Crowborough, UK, 1993, p. 177.
[4] J.Y. Huot, in A.J. Salkind, F.R. McLarnon and V.S. Bagotzky (eds.), *Proc. Electrochem. Soc. Rechargeable Zinc Batteries, 95-14*, 1996, p. 22.
[5] J. Daniel-Ivad and J.Y. Huot, in A.J. Salkind, F.R. McLarnon and V.S. Bagotzky (eds.), *Proc. Electrochem. Soc. Rechargeable Zinc Batteries, 95-14*, 1996, p. 109.
[6] P.G. Cheeseman and M.G. Stock, in L.J. Pearce (ed.), *Power Sources 10*, International Power Sources Symposium, Crowborough, UK, 1985, p. 217.
[7] R.F. Scarr and J.C. Hunter, in D. Linden (ed.), *Handbook of Batteries*, McGraw-Hill, New York, 2nd edn., 1995, Ch. 10.
[8] J.T. West and F.F. Bonacker, *IECEC Conf. Proc., 1995*, p. 255.
[9] H. Yoshizawa and A. Miura, *Prog. Batteries Battery Mater., 12* (1993) 132.
[10] R.N. Esdale, N.A. Hampson, P.C. Jones and A.N. Strachan, *J. Appl. Electrochem., 1* (1971) 213.
[11] H.E. Brown, *Zinc Oxide Rediscovered*, The New Jersey Zinc Co., New York, 1957, p. 32.
[12] G. Dubé, R. Renaud and J.Y. Huot. *Prog. Batteries Battery Mater., 10* (1991) 151.